Early and late stage of neurodegeneration induced by trimethyltin in hippocampus and cortex of male Wistar rats

Zdenka Gasparova [1], Pavol Janega [2,3], Veronika Stara [1], Eduard Ujhazy [1]

1 Institute of Experimental Pharmacology and Toxicology, Slovak Academy of Sciences, Bratislava, Slovak Republic
2 Department of Pathology, Faculty of Medicine, Comenius University, Bratislava, Slovak Republic
3 Institute of Normal and Pathological Physiology, Slovak Academy of Sciences, Bratislava, Slovak Republic

Correspondence to: Assoc. Prof. Eduard Ujhazy, CSc.
Institute of Experimental Pharmacology and Toxicology,
Slovak Academy of Sciences,
Dubravska cesta 9, Bratislava, SK-84104, Slovak Republic.
TEL: +421 259410674; E-MAIL: eduard.ujhazy@savba.sk

Submitted: 2012-11-12 Accepted: 2012-11-20 Published online: 2012-12-01

Key words: **rat; hippocampus; cortex; neurodegeneration; trimethyltin; neurotransmission; apoptosis; protein carbonyl groups**

Neuroendocrinol Lett 2012; **33**(7):689–696 **PMID:** 23391880 NEL331012A06

Abstract

BACKGROUND: Trimethyltin (TMT), a potent neurotoxicant, elicits neuronal death in the limbic system and causes damage particularly in the hippocampus. Current interest relates to the opportunity to use TMT as an experimental model of neurodegeneration in the study of Alzheimer-like diseases.

OBJECTIVE: In light of recently found species-specific and strain-specific differences in TMT intoxication, the aim of this study was to characterise the model of TMT-induced neurodegeneration in the brain of Wistar rats during early (days 1–3) and late (days 22–24) stage of neuronal damage.

RESULTS: Reduced neurotransmission at the CA3–CA1 synapse and reduced number of cells accompanied with reduced width of CA1 pyramidal cell layer were observed at the late stage of TMT intoxication (7 mg/kg, *i.p.*). Long-term potentiation of excitatory postsynaptic potential, elicited by train stimulation (100 Hz, 1s), was not impaired by the dose of TMT tested. Activation of pro-apoptotic caspase-3 suggests involvement of apoptosis in neuronal cell death in the hippocampus at the late stage of TMT intoxication. Increased protein carbonyl formation was proved in the cortex at the early stage of TMT intoxication compared both to controls in the early and late stage and to the late stage of TMT action.

CONCLUSIONS: TMT-induced neurodegeneration was proved in the brain of Wistar rats. Changes found in the parameters examined may be reliable indicators of neurodegeneration. The increased level of carbonyls in the cortex at the early stage indicates that particularly at the onset of progressive neurodegeneration compounds with antioxidative properties may be effective in slowing down brain injury.

Abbreviations:

DAB	- diaminobenzidine	HFS	- high frequency stimulation
DMSO	- dimethyl sulfoxide	LTP	- long-term potentiation
fEPSP	- field excitatory postsynaptic potential	PBS	- phosphate-buffered physiological salt solution
HE	- haematoxylin and eosin	TMT	- trimethyltin

ORIGINAL ARTICLE

INTRODUCTION

Trimethyltin chloride (C_3H_9ClSn) (TMT) is an intermediate by-product in the production of some tin compounds, which have a broad application in agriculture, e.g. biocides, and in industry, e.g. PVC heat stabilisers. TMT is a strong toxin. In human victims TMT contamination was manifested by hearing loss, disorientation, confabulation, amnesia, aggressiveness, hyperphagia, complex partial and tonic-clonic seizures, nystagmus, ataxia, and mild sensory neuropathy. TMT as a potent neurotoxicant elicits neuronal death in both the human and animal limbic system and causes severe damage, particularly in the hippocampus. Thus current interest in TMT does not relate to environmental toxicology but rather to the opportunity to use TMT as an important research aid for the study of brain function (Geloso *et al.* 2011; Koczyk 1996). The pathology elicited by TMT-induced neurodegeneration is common to most neurodegenerative disorders, like neuronal cell death and cognitive impairment. TMT has been found useful as experimental model in the study of Alzheimer-like diseases (Ishikawa *et al.* 1997; Nilsberth *et al.* 2002). The primary target for TMT is the hippocampus where it exerts its toxic effects on pyramidal neurons. Structural damage starts to be observed 2–3 days after TMT administration, becomes evident within 21 days, and continues during further several weeks (Whittington *et al.*1989). The delayed onset and prolonged duration are likely due to the high affinity of rat haemoglobin for TMT. Haemoglobin may therefore serve as a reservoir slowly and continuously releasing TMT into the plasma, from which it then enters the brain (Rose and Aldridge 1968). TMT is demethylated to dimethyltin which binds irreversibly to a protein called stannin. Stannin may be localised in the outer mitochondrial (Billingsley *et al.* 2006) and endoplasmatic reticulum membrane (Davidson *et al.* 2004). The TMT-induced effect includes its cytotoxic action directly on glial cells, where an increase in levels of glial fibrilary acidic protein was observed (Richter-Landsberg and Besser, 1994) along with changes in Na^+-K^+-ATPase activity and ion permeability, resulting from swelling of primary cultures of astrocytes (Ashner and Ashner, 1992). TMT was found to disregulate Ca^{2+} homeostasis and increase intracellular calcium levels (Piacentini *et al.* 2008). Increased formation of reactive oxygen species, reactive nitrogen species and apoptotic changes may explain the mechanism of the neurotoxic action of TMT (Harry *et al.* 2001; Viviani *et al.* 2001).

Species-specific differences were found in TMT-induced neurodegeneration between rat and mouse (Trabucco *et al.* 2009). While in mice TMT selectively damaged dentate gyrus granule cells acutely within the first three days (Chang *et al.* 1982), neurodegeneration in rats proved to be progressive, developing over more than 3 weeks and affecting mainly CA1 and CA3 pyramidal neurons (Chang, 1986). The LD_{50} dose in white Wistar rats (Porton strain) was determined at 12.6 mg/kg (Brown *et al.* 1979), while in mice it was found to be about 1.7 mg/kg (Maurice *et al.* 1999). The influence of the rat strain was evident in TMT intoxication in Long-Evans and Fischer 344 rats (Chang *et al.* 1983; Gordon and Fogelson, 1991; Moser, 1996). Bearing in mind the species-specific and putative strain-specific differences indicated in TMT-induced neurodegeneration, in the present study we characterised several features of the early and late stage of neurodegeneration in the TMT model in the hippocampus and cortex of Wistar male rats, as a basis for future studies of the effect of novel neuroprotective compounds in Alzheimer-like diseases. The aims were to determine: 1) the neurotransmission strength and synaptic plasticity at the CA3–CA1 synapse, 2) protein carbonyl formation in cortex homogenates, and 3) morphometrical changes in the CA1 area and immunohistochemically apoptosis in the hippocampus during the early and late stage of brain degeneration of male Wistar rats exposed to TMT (7mg/kg, *i.p.*), in comparison to control rats receiving saline (0.9% NaCl, *i.p.*). The authors of the present work selected the early stage of TMT-induced neurodegeneration (days 1–3) on the basis of reported changes of a plethora of biochemical parameters within the first days after TMT administration (Shin *et al.* 2005), and the late stage of TMT-induced neurodegeneration (days 22–24) on the basis of reported structure damage evident within 21 days in the rat hippocampus (Brock and O'Callaghan 1987; Whittington *et al.* 1989).

MATERIAL AND METHODS

Animals and TMT administration

Male Wistar rats were used from the breeding station Dobra Voda (Slovak Republic, reg. No. SK CH 24011). Rats (weight 210–230 g, age 10–12 weeks, n=24) had free access to water and food pellets and were kept on a 12h/12 h light/dark cycle. All procedures involving animals were performed in compliance with the Principles of Laboratory Animal Care issued by the Ethical Committee of the Institute of Experimental Pharmacology and Toxicology, Slovak Academy of Sciences and by the State Veterinary and Food Administration of Slovakia. TMT chloride (Sigma-Aldrich) dissolved in 0.1% dimethyl sulfoxide (DMSO) and in sterile saline just prior to application, was administered in a single dose of 7 mg/kg of body weight *intraperitoneally* in the volume of 0.3 ml/100 g of body weight. Control rats received an equal volume of sterile saline with 0.1% DMSO. Both experimental groups of animals, controls and TMT, were further divided into two subgroups, where the animals were pooled due to the time courses for termination as follows: days 1–3 after TMT /or saline administration for the early neurodegeneration stage and days 22–24 after TMT /or saline administration for the late neurodegeneration stage, with six animals in each subgroup. Electrophysiologi-

cal measurements were performed on the left hippocampus of each rat decapitated on day 1, 2, 3, 22, 23 and 24 after TMT /or saline administration. In light of electrophysiological experiments which could be performed only on one hippocampus/one rat/day, TMT was administered to 6 rats one week after saline had been administered to the first 6 rats. Five weeks later, the same protocol of experiment was repeated on further 12 rats (saline *n*=6, TMT *n*=6). Morphometrical and immunohistochemical determinations were performed on the right hippocampus (whole right hemisphere was cut) of each rat decapitated on days as mentioned above. Biochemical statement of protein carbonyl groups were performed on the cortex of the left hemisphere of each rat *per* sample. Data were cumulated from days 1, 2 and 3 in the first and second batch of experiments to define neurodegeneration in the early stage, and from days 22, 23 and 24 to define neurodegeneration in the late stage by all kinds of experimental approaches used.

Preparation of rat hippocampal slices and extracellular recording

The rats were shortly anaesthetised by ether, decapitated and the hippocampus was quickly removed from the brain and cut into transversal 400 μm thick slices with the McIllwain Tissue Chopper (Stoelting, USA). The slices were kept in the holding chamber for 60–80-min recovery period before the experiment started. During the measurement, one slice was kept in the recording chamber and continuously perfused with artificial cerebrospinal fluid saturated with 95% O_2 and 5% CO_2 at a constant rate monitored by aquatic manometer. The temperature of the recording chamber was kept at 33.0–34.0 °C. Electrically evoked responses were recorded by DigiData 1322A (Molecular Devices, Axon Instruments, USA) with sampling rate 10 kHz and stored on personal computer for off-line analysis by the AxoScope10.2 software. Initial slope and magnitude of field excitatory postsynaptic potential (fEPSP) were recorded extracellularly in the *stratum radiatum* of CA1 pyramidal neurons in response to electric stimulation of Schäffer collaterals in rats exposed to TMT and then compared to responses of control rats. Input-output curves were prepared using electrical stimuli with increasing intensity from 5 to 15 V, with stimulus duration of 100 μs, at stimulus frequency of 0.05 Hz. The same stimulus intensity was repeated five times at the same slice and means ± S.E.M. were calculated from 6–7 slices in each experimental group consisting of six rats. Before induction of high frequency stimulation (HFS), the baseline response was adjusted as follows: at the point when a population spike generation started to be detected, the stimulus intensity was reduced to obtain about 50% of the previous fEPSP amplitude. Then the slice was stabilised for 15–20 min and baseline response was recorded. Long-term potentiation (LTP) was induced by HFS of a single 100-Hz train with 1-s train duration. After HFS, the baseline stimulation frequency of 0.05 Hz continued for at least 60 min.

Protein carbonyl formation in rat brain cortex

Protein carbonyl formation was determined by the method of Levine and co-workers (1990), modified by Blackburn and co-workers (1999), where 2,4-dinitrophenylhydrazine reacts with the protein carbonyl group and protein hydrazon is generated, which is detected spectrophotometrically with absorbance maximum at 360–370 nm. Proteins were detected spectrophotometrically in the same sample at 280 nm. Homogenate (10%) of the rat brain cortex was used. Basal level of protein carbonyl groups at the early and late stage of degeneration in the model of TMT-induced neurodegeneration was compared with appropriate controls.

Width and cell number of CA1 pyramidal cell layer in rat hippocampus

The right hemisphere of the brain was fixed in 4% formaldehyde after decapitation of the rat. The oblique sagittal section of the brain in the midline was processed, embedded in paraffin and cut to obtain slices across the hippocampus. Brain slices, 4 μm thick, were routinely stained by haematoxylin and eosin (HE). The CA1 area in the hippocampus was selected and captured by optical microscope (Leica DM 2000, Wetzlar, Germany) with attached camera (S50, Canon, Japan), using the final magnification 400x in three microscopic fields. The width of the pyramidal cell layer in the CA1 area, expressed in micrometers, was determined at three places in each captured microscopic field by digital morphometry using ImageJ software (1.46b, National Institutes of Health, USA) (Abramoff *et al.* 2004). The number of the cells in the CA1 area was counted in each captured field and expressed as percentage compared to the control group.

Immunohistochemical assessment of apoptosis

Fixed brain tissue samples were routinely processed for immunohistochemistry. The 4 μm thick slices were deparaffinised and rehydrated in phosphate-buffered physiological salt solution (PBS). Before immunohistochemical analysis, microwave epitope retrieval was performed on slides stained with anti-cleaved caspase-3 and with anti-Bax (10mmol/l citrate buffer, pH 6.0). The slides were subsequently incubated overnight with polyclonal rabbit anti-cleaved caspase-3 (Cell Signaling, Danvers, USA) diluted 1:300 and with polyclonal rabbit anti-Bax (Dako, Glostrup, Denmark) diluted 1:100. The antibodies were diluted in Dako Real antibody diluent (Dako, Glostrup, Denmark). After 3 rinsing steps of 5 minutes each in PBS, the sections were incubated for 30 minutes with Histofine mouse and rabbit antibody polymer conjugated with horse radish peroxidase (Nichirei Biosciences, Tokyo, Japan). After 3 rinsing steps of 5 minutes each in PBS, the peroxidase activity was visualised with diaminobenzidine (DAB;

Dako, Glostrup, Denmark). Subsequently the sections were counterstained with haematoxylin. The positivity of each protein was evaluated in light microscope (Leica DM 2000, Wetzlar, Germany). The intensity of Bax expression was evaluated in the CA1 area by morphometry using the ImageJ software (1.46b, National Institutes of Health, USA) (Abramoff *et al.* 2004). Results are expressed as ratio of protein positivity area (characteristic brown colour in DAB staining) to the analysed CA1 area. The nuclear positivity of cleaved caspase-3 was counted as the number of positive nuclei in CA1 area and expressed as percentage compared to the control group.

Statistical evaluation

The results were analysed statistically by one-way ANOVA using GraphPad Prism Software (GraphPad, La Jolla, USA) or by the Student t-test. The limit of $p<0.05$ was considered statistically significant. The values were expressed as mean ± SEM.

RESULTS

Recordings of electrically evoked field excitatory postsynaptic potentials (fEPSPs) were analysed in hippocampal slices of rats exposed to a single dose of TMT (7 mg/kg of body weight, *i.p.*). Responses were monitored at the early (days 1–3) and the late (days 22–24) stage of TMT-induced neurotoxicity and compared with the appropriate group of control rats receiving saline. Evoked fEPSP was elicited by electrical stimulation of Schäffer collaterals by intensities from 5 to 15 V of stimulus duration of 100 μs. Both the reduced fEPSP amplitude and reduced initial slope of fEPSP recorded in the *stratum radiatum*, plotted as a function of stimulus intensity, were obtained in the hippocampus of rats decapitated at the late stage of TMT action compared to control rats. Input-output curves are shown in Figure 1. Normalised LTP amplitude, expressed as the fEPSP magnitude or as the fEPSP initial slope of response measured during 51–60 min after HFS (100 Hz, 1s) did

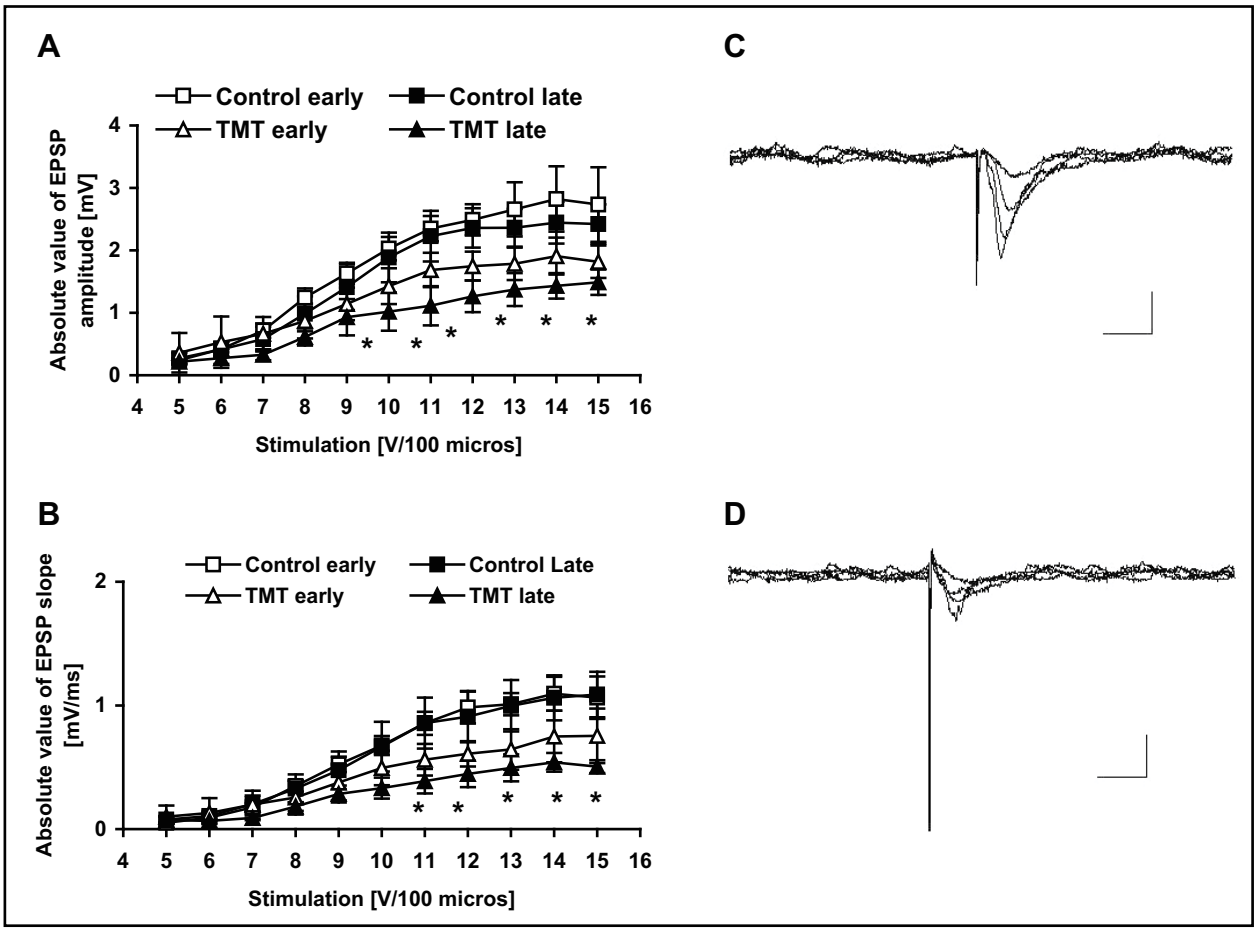

Fig. 1. Changes of the excitatory postsynaptic potential (EPSP) in the hippocampal CA1 area of TMT-exposed rats. Responses evoked by electrical stimulation of Schäffer collaterals were recorded extracellularly at *the stratum radiatum* of the CA1 area. (**A**) EPSP amplitude, and (**B**) initial slope of EPSP were significantly reduced at the late stage of TMT-induced neurodegeneration (22–24 days after TMT administration; 7 mg/kg, *i.p.*) compared to control rats obtaining saline. At the early stage of TMT-induced neurodegeneration (1–3 days after TMT administration), a non-significant reduction of EPSP amplitude and initial slope is seen. Values are means ± S.E.M. Statistical differences were calculated by the Student t-test, where *$p<0.05$. Representative responses from the hippocampus of a control rat (**C**) compared to responses of a rat at the late stage of TMT-induced neurodegeneration (**D**), both induced by equipotent stimulation. Insert calibration: horizontally 10 ms, vertically 1 mV.

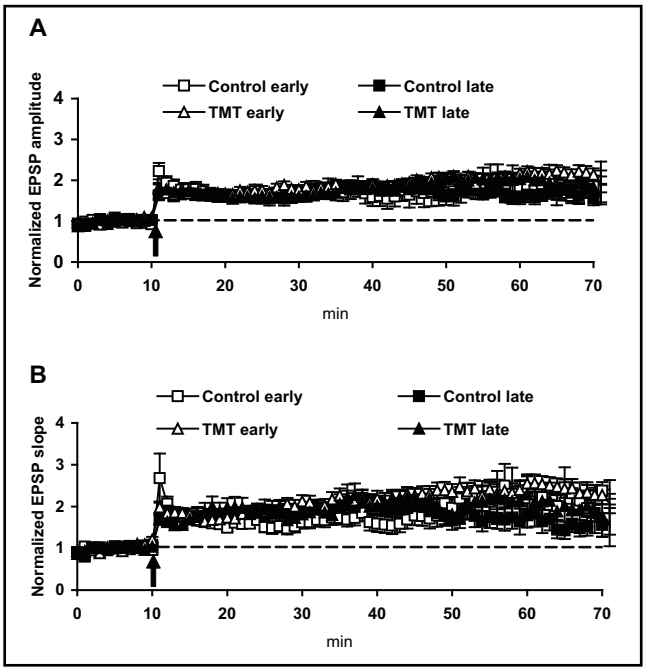

Fig. 2. Long-term potentiation (LTP) of neurotransmission at the CA3-CA1 synapse in rat hippocampus. Despite reduced basal neurotransmission in the hippocampus of TMT-exposed rats (absolute values are shown in Figure 1), LTP induction and its maintenance were not changed either during the early or late stage of TMT-induced neurodegeneration, presumably due to the dose of TMT tested (7 mg/kg *i.p.*). Relative magnification of excitatory postsynaptic potential (EPSP) amplitude (**A**) and initial slope of EPSP (**B**) due to a single train of high frequency stimulation (100 Hz, 1s) did not differ in the hippocampus of TMT-exposed rats and controls. Values are means ± S.E.M.

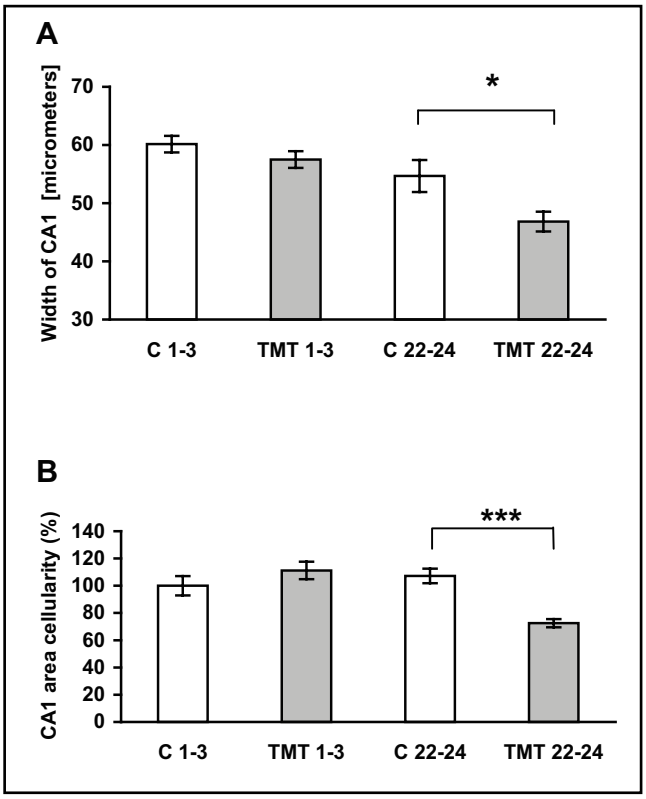

Fig. 3. Width and cell number in the CA1 pyramidal cell layer. (**A**) Reduced width of CA1 pyramidal cell layer was observed during the late stage of TMT-induced neurodegeneration in rats exposed to a single dose of TMT (7 mg/kg; *i.p.*) compared to controls and this was accompanied by (**B**) reduced cell number in the CA1 pyramidal cell layer. Values are means ± S.E.M. Statistical differences were calculated by ANOVA, where $*p<0.05$, $***p<0.001$.

not significantly differ in the rat hippocampus exposed to TMT either at the early or late stage of TMT-induced neurodegeneration, compared to controls (Figure 2). Thus induction and maintenance of LTP was not impaired in the hippocampus of TMT-exposed rats due to the dose of TMT tested. The relation between reduced basal neurotransmission found at the late stage of TMT-induced neurotoxicity and morphological changes in the hippocampus was studied. The width of the CA1 pyramidal cell layer and cellularity index of the CA1 pyramidal cell layer was determined in HE stained hippocampal sections. Morphometrical analyses revealed a significant reduction of the pyramidal cell layer width characterized by the reduction of the cell number in the CA1 area after 22–24 days of TMT administration compared to controls (Figure 3). This reduction was accompanied by marked caspase-3 positivity in the CA1 area of rat hippocampal sections during the late stage of TMT-induced neurodegeneration proved by immunohistochemistry (Figure 4). No changes of Bax positivity was found neither in the early nor late stage of TMT-induced neurotoxicity. Protein damage in the rat cortex due to the TMT action was assessed by the determination of protein carbonyl formation. The baseline level of protein carbonyl groups in the cortex of controls sacrified on days 1–3 was similar to that of controls sacrified on days 22–24. The baseline level of protein carbonyls was significantly higher in the cortex of rats exposed to a single dose of TMT during the early stage of TMT-induced neurodegeneration compared to both control groups as well as to the group of rats during the late stage of TMT action (Figure 5).

DISCUSSION

Recently it has been accepted that distinct brain regions differ by the degree of sensitivity to cellular stress (Cervos-Navarro and Diemer, 1991; Pulsinelli and Brierley, 1979; Schmidt-Kastner *et al.* 1990). Selective neuronal death was observed in certain most vulnerable regions of the CNS, in particular in the CA1 area of the hippocampus. Aging, brain ischaemia, neurodegeneration and also the TMT-induced hippocampal neurodegeneration used as a model of Alzheimer-like disease resemble in some pathogenetic mechanisms, including enhanced vulnerability of the CA1 area (Geloso *et*

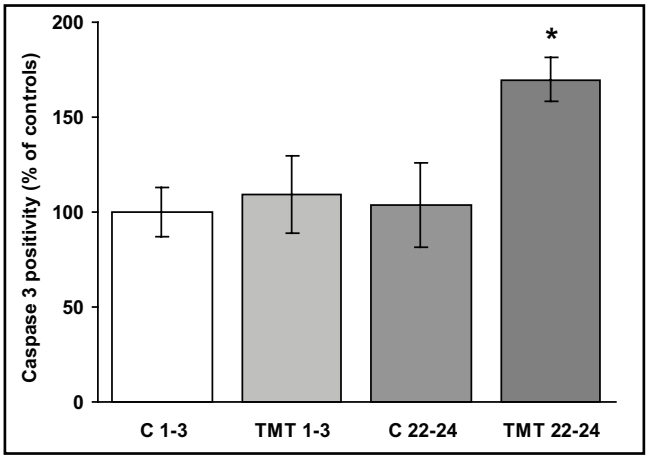

Fig. 4. Caspase-3 positivity in rat hippocampus. Activation of caspase-3 during the late stage of TMT action was determined immunohistochemically in the slides incubated overnight with polyclonal rabbit anti-cleaved caspase-3. Values are means ± S.E.M. Statistical difference was calculated by ANOVA, where **p*<0.05.

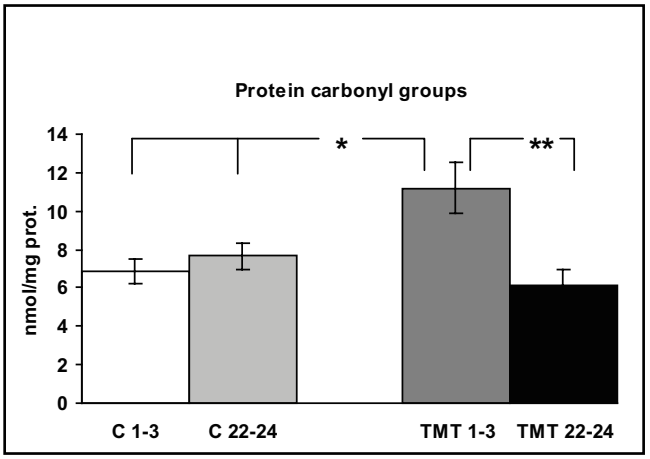

Fig. 5. Level of protein carbonyl groups in the rat cortex. Increased protein carbonylation is seen in the early stage of TMT-induced neurodegeneration. Values are means ± S.E.M. Statistical differences were calculated by Student t-test, where **p*<0.05 and ***p*<0.01.

al. 2011; Jackson *et al.* 2009; Larsson *et al.* 2001). Our results confirmed the CA1 vulnerability in the model of TMT-induced neurodegeneration by electrophysiological and morphometrical approaches in Wistar rats. Both reduced synaptic transmission at the CA3–CA1 synapse and reduced width of the CA1 pyramidal cell layer accompanied by reduced cell number was observed in the hippocampus of TMT-exposed Wistar rats during the late stage of intoxication. There are only few literary sources studying electrophysiological responses to determine the TMT action on neuronal function in the hippocampus and these works were focused mainly on the bath application of TMT (Armstrong *et al.* 1987; Janigro and Costa 1987; Krüger *et al.* 2005; Melani *et al.* 2005). A large reduction of population spike magnitude (Armstrong *et al.* 1987; Melani *et al.* 2005) and decreased amplitudes of evoked excitatory postsynaptic potentials (Krüger *et al.* 2005) were reported due to *in vitro* TMT application. The presented results of reduced synaptic transmission found in the hippocampus of Wistar male rats which received TMT *intraperitoneally* are in good agreement with *in vitro* data. Despite reduced basal neurotransmision in the hippocampus of TMT-exposed rats, the presented data showed unaffected induction and holding of LTP after HFS at the CA3–CA1 synapse in TMT intoxicated rats (7 mg/kg; *i.p.)* compared to control rats (saline; *i.p.).* By contrast, inhibited induction and maintenance of LTP recorded from the CA1 dendritic region was reported by application of TMT *in vitro* (Krüger *et al.* 2005). Such a discrepancy suggests that systemic administration and acute bath application of TMT may differ in the mechanism of neurotoxicant action on synaptic plasticity.

It has been generally accepted that apoptosis occurs under various pathologic and physiologic conditions (Kerr *et al.* 1972; Migheli *et al.* 1994). The mechanisms of cellular death involved in TMT-induced neurodegeneration have not yet been fully clarified. On the basis of experiments *in vitro*, Gunasekar and coworkers (2001) concluded that low concentrations of TMT (0.01–0.1 μmol/l) caused apoptotic cell death and high concentrations of TMT initiated necrotic death. Recently it was demonstrated that TMT produced a time- and concentration-dependent apoptotic death on an immortalised hippocampal neuronal cell line (HT-22 cell), which was caspase-mediated (Zhang *et al.* 2006). Caspase-3 plays a pivotal role in apoptotic processes. Focus on the way of neuronal death suggests that the model of TMT-induced neurodegeneration is associated with apoptotic neuronal death rather than with necrosis. Geloso and coworkers (2002) presented data showing that TMT induced the apoptotic form of cell death in adult mice, accompanied by the expression of both activated caspase-3 and COX-2 in the degenerating granular cells. The presence of marked caspase-3 positivity reported here also suggests that apoptosis may contribute to neuronal cell death and to functional and morphological differences at the CA3–CA1 synapse observed in the late stage of TMT-induced intoxication in adult male Wistar rats. Contrary to the observation of Zhang and coworkers (2006) on hippocampal cell line, the presented data showed that the Bax pathway was probably not involved in the *in vivo* model of TMT neurodegeneration.

Age-associated increase in protein oxidation and reactive oxygen species production in the cerebral cortex and hippocampus of aged rats were reported (Balu *et al.* 2005). Oxidative damage may be one of the earliest events in the onset and progression of Alzheimer`s disease. Similarly, 1-methyl-4-phenyl-1,2,3,6-tetrahydro-

pyridine toxicity elicited by a neurotoxin that induces a Parkinsonian-type syndrome in animals, partially depends on the production of free radicals which play a key role in the apoptotic death of neurons (Ortiz *et al.* 2001). An increased level of protein carbonylation was found in neurodegenerative disorders and this level correlated with cognitive impairment (Keller *et al.* 2005). In the model of TMT-induced neurodegeneration, an increased generation of cellular oxidative species was reported in a number of different cell lines and primary cells (Gunasekar *et al.* 2001; Jenkins and Barone, 2004; Mundy and Freudenrich, 2006) and in the hippocampus of Sprague-Dawley rats (Shin *et al.* 2005). The increased baseline level of the content of protein carbonyls on days 1–3 of TMT-induced intoxication found here suggests oxidative damage at the early stage of TMT-induced neurodegeneration.

In conclusion, TMT-induced neurodegeneration was found in the hippocampus and cortex of Wistar rats. Changes determined in the parameters examined may be reliable indicators of neurodegenerative impairment. The increased level of the content of protein carbonyl groups at the early stage of TMT-induced neurodegeneration indicates an arising chance that particularly at the onset of progressive neurodegenerative Alzheimer-like diseases, compounds with antioxidative properties may prove effective in slowing down brain injury.

ACKNOWLEDGEMENTS

This study was supported by the VEGA grants no. 2/0048/11 and 2/0081/11. The authors thank Mrs. Julia Polakova and Mr. Lucian Revak for technical assistance.

REFERENCES

1 Abramoff MD, Magalhaes PJ, Ram SJ (2004). Image Processing with ImageJ, Biophotonics Internat. **11:** 36–42
2 Armstrong DL, Read HL, Cork AE, Montemayor F, Wayner MJ (1987). Effetcs of trimethyltin on evoked potentials in mouse hippocampal slices. Neurotoxicol Teratol. **9:** 359–362.
3 Ashner M, Ashner JL (1992). Cellular and molecular effects of trimethyltin and triethyltin: relevance to organotin neurotoxicity. Neurosci Behav Rev. **16:** 427–435.
4 Balu M, Sangeetha P, Murali G, Panneerselvam C (2005). Age-related oxidative protein damages in central nervous system of rats: modulatory role of grape seed extract. Int J Dev Neurosci. **23:** 501–507
5 Billingsley ML, Yun J, Reese BE, Davidson CE, Buck-Koehntop BA, Veglia A (2006). Functional and structural properties of stannin: roles in cellular growth, selective toxicity, and mitochondrial responses to injury. J Cell Biochem. **98:** 243–250.
6 Blackburn AC, Doe WF, Buffinton GD. (1999). Protein carbonyl formation on mucosal proteins *in vitro* and in dextran sulfate-induced colitis. Free Radic Biol Med. **27:** 262–270.
7 Brock TO, O'Callaghan JP (1987). Quantitative changes in the synaptic vesicle proteins synapsin I and p38 and the astrocyte-specific protein glial fibrillary acidic protein are associated with chemical-induced injury to the rat central nervous system. J Neurosci. **7:** 931–942.
8 Brown AW, Aldridge WN, Street BW, Verschoyle RD (1979). The behavioural and neuropathologic sequelae of intoxication by trimethyltin compound in the rat. Am J Pathol. **97:** 59–81.
9 Cervos-Navarro J, Diemer NH (1991). Selective vulnerability in brain hypoxia. Crit Rev Neurobiol. **6:** 149–182.
10 Chang LW (1986). Neuropathology of trimethyltin: a proposed pathogenetic mechanism. Fundam Appl Toxicol. **6:** 217–232
11 Chang LW, Tiemeyer TM, Wenger GR (1982). Neuropathology of mouse hippocampus in acute trimethyltin intoxication. Neurobehav Toxicol Teratol. **4:**149–156.
12 Chang LW, Wenger GR, McMillan DE, Dyer RS (1983). Species and strain comparison of acute neurotoxic effects of trimethyltin in mice and rats. Neurobehav Toxicol Teratol. **5:** 337–350.
13 Davidson CE, Reese BE, Billingsley ML, Yun JK (2004). Stannin, a protein that localizes to the mitochondria and sensitizes NIH-373 cells to trimethyltin and dimethyltin toxicity. Mol Pharmacol. **66:** 855–863.
14 Geloso MC, Corvino V, Michetti F (2011). Trimethyltin-induced hippocampal degeneration as a tool to investigate neurodegenerative processes. Neurochem. Int. **58:** 729–738.
15 Geloso MC, Vercelli A, Corvino V, Repici M, Boca M, Haglid K, Zelano G, Michetti F (2002) Cyclooxygenase-2 and Caspase 3 Expression in Trimethyltin-Induced Apoptosis in the Mouse Hippocampus. Exp Neurology .**175:** 152–160.
16 Gordon CJ, Fogelson L (1991). Comparison of rats of the Fischer 344 and Long-Evans strains in their autonomic thermoregulatory response to trimethyltin administration. J Toxicol Environ Health. **32:** 141–152.
17 Gunasekar PG, Li L, Prabhakaran K, Eybl V, Borowitz JL, Isom GE (2001). Mechanisms of the apoptotic and necrotic actions of trimethyltin in cerebellar granule cells. Toxicol Sci. **64:** 83–89.
18 Harry GJ, Sills R, Schlosser MJ, Maier WE (2001). Neurodegeneration and glia response in rat hippocampus following nitro-L-arginine metyl ester (L-NAME). Neurotoxicol Res. **3:** 307–3019.
19 Ishikawa K, Kubo T, Shibanoki S, Matsumoto A, Hata H, Asai S (1997). Hippocampal degeneration inducing impairment of learning in rats: model of dementia? Behav Brain Res. **83:** 39–44.
20 Jackson TC, Rani A, Kumar A, Foster TC (2009). Regional hippocampal differencies in AKT survival signaling across the lifespan: implications for CA1 vulnerability with aging. Cell Death Differ. **16:** 439–448.
21 Janigro D, Costa LG (1987). Effetcs of trimethyltin on granule cells excitability in the *in vitro* rat dentate gyrus. Neurotoxicol Teratol. **9:** 33–38.
22 Jenkins SM, Barone S (2004). The neurotoxicant trimethyltin induced apoptosis via caspase activation, p38 protein kinase, and oxidative stress in PC12 cells. Toxicol Lett. **147:** 63–72.
23 Keller JN, Schmitt FA, Scheff SW, Ding Q, Chen Q, Butterfield DA, Markesbery WR (2005). Evidence of increased oxidative damage in subjects with mild cognitive impairment. Neurology. **64**: 1152–1156**.**
24 Kerr JF, Wyllie AH, Currie AR (1972). Apoptosis: a basic biological phenomenon with wide-ranging implications in tissue kinetics. Br J Cancer **26:** 239–257.
25 Koczyk D (1996). How does trimethylthin affect the brain: facts and hypotheses. Acta Neurobiol Exp. **56:** 587–596.
26 Krüger K, Diepgrond V, Ahnefeld M, Wackerbeck C, Madeja M, Binding N, Musshoff U (2005). Blockade of glutamatergic and GABAergic receptor channels by trimethyltin chloride. Br J Pharmacol. **144:** 283–292.
27 Larsson E, Lindvall O, Kokaia Z (2001). Stereological assessment of vulnerability of immunocytochemically identified striatal and hippocampal neurons after global cerebral ischemia in rats. Brain Res. **913:** 117–132.
28 Levine RL, Garland D, Oliver CN, Amici A, Climent I., Lenz AG, Ahn BW, Shaltiel S, Stadtman ER. (1990). Determination of carbonyl content in oxidatively modified proteins. Methods Enzymol. **186:** 464–478.
29 Maurice T, Phan VL, Noda Y, Yamada K, Privat A, Nabeshima T (1999). The attenuation of learning impairments induced after exposure to CO or trimethyltin in mice by sigma receptor ligands involves both sigma1 and sigma2 sites. Br J Pharmacol. **127:** 335–342.

30 Melani R, Rebaudo R, Noraberg J, Zimmer J, Balestrino M (2005). Changes in extracellular action potential detect kainic acid and trimethyltin toxicity in hippocampal slice preparations earlier than MAP2 density measurements. Altern Lab Anim. **33:** 379–386.
31 Migheli A, Cavalla P, Marino S, Schiffer D (1994). A study of apoptosis in normal and pathologic nervous tissue after in situ end-labeling of DNA strand breaks. J Neuropathol Exp Neurol. **53:** 606–616.
32 Moser VC (1996). Rat strain- and gender-related differences in neurobehavioral screening: acute trimethyltin neurotoxicity. J Toxicol Environ Health. **47:** 567–586.
33 Mundy WR, Freudenrich TM (2006). Apoptosis of cerebellar granule cells induced by organotin compounds found in drinking water: involvement of MAP kinases. Neurotoxicology. **27:** 71–81.
34 Nilsberth C, Kostyszyn B, Luthman J (2002). Changesin APP; PS1 and other factors related to Alzheimer´s disease pathophysiology after trimethyltin-induced brain lesion in the rat. Neurotoxicol Res. **4:** 625–636.
35 Ortiz GG, Crespo-López ME, Morán-Moguel C, García JJ, Reiter RJ, Acuna-Castroviejo D (2001). Protective role of melatonin against MPTP-induced mouse brain cell DNA fragmentation and apoptosis *in vivo*. Neuro Endocrinol Lett. **22:** 101–108.
36 Piacentini R, Gangitano C, Ceccariglia S, Del Fà A, Azzena GB, Michetti F, Grassi C (2008). Dysregulation of intracellular calcium homeostasis is responsible for neuronal death in an experimental model of selective hippocampal degeneration induced by trimethyltin. J Neurochem. **105:** 2109–2121.
37 Pulsinelli WA, Brierley JB (1979). A new model of bilateral hemispheric ischemia in the unanesthetized rat. Stroke **10:** 267–272
38 Richter-Landsberg C, Besser A (1994). Effects of organotins on rat brain astrocytes in culture. J. Neurochem. **63:** 2202–2209.
39 Rose MS, Aldridge WM (1968). The interaction of triethyltin with components of animal tissue. Biochem J. **106:** 821–826.
40 Schmidt-Kastner R, Ophoff BG, Hossmann KA (1990). Pattern of neuronal vulnerability in the cat hippocampus after one hour of global cerebral ischemia. Acta Neuropathol. **79:** 445–455.
41 Shin EJ, Suh SK, Lim YK, Jhoo WK, Hjelle OP, Ottersen OP, Shin CY, Ko KH, Kim WK, Kim DS, Chun W, Ali S, Kim HC (2005). Ascorbate attenuates trimethyltin-induced oxidative burden and neuronal degeneration in the rat hippocampus by maintaining glutathione homeostasis. Neuroscience. **133:** 715–727.
42 Trabucco A, Di Pietro P, Nori SL, Fulceri F, Fumagalli L, Paparelli A, Fornai F (2009). Methylated tin toxicity a reappraisal using rodents models. Arch It Biol. **147:** 141–153.
43 Viviani B, Corsini E, Pesenti M, Galli CL, Marinovich M (2001). Trimethyltin-activated cyclooxygenase stimulates tumor necrosis factor-alpha release from glial cells through reactive oxygen species. Toxicol Appl Pharmacol. **172:** 93–97.
44 Whittington DL, Woodruff ML, Baisden RH (1989). The time-course of trimethyltin-induced fiber and terminal degeneration in hippocampus. Neurotoxicol Teratol. **11:** 21–33.
45 Zhang L., Li L., Prabhakaran K., Borowitz JL., Isom GE (2006) Trimethyltin-induced apoptosis is associated with upregulation of inducible nitric oxide synthase and Bax in a hippocampal cell line. Toxicol Appl Pharmacol. **216:** 34–43